WILEY | Hindawi

Research Article

Protective Activity of Alpha-Mangostin against UVB-Induced Injury in HaCaT Cells by Modulating the Ceramide and MAPK and NF-*κ*B Signaling Pathways

Jiahui Jin,[1,2] **Yan Bao,**[3] **Yan Wang** ⓘ **,**[1,2] **Huimin Zheng,**[1,2] **Hao Guo,**[4] **Lei Zhang,**[4] **Ruoxi Guo,**[4] **and Lei Yang** ⓘ [5]

[1]*State Key Laboratory of Component-Based Chinese Medicine, Tianjin University of Traditional Chinese Medicine, Tianjin, China*
[2]*Haihe Laboratory of Tianjin University of Traditional Chinese Medicine, Tianjin University of Traditional Chinese Medicine, Tianjin, China*
[3]*Tianjin Stomatological Hospital, The Affiliated Stomatological Hospital of Nankai University, Tianjin, China*
[4]*R&D Department, Tianjin Shangmei Cosmetics Co., Ltd, Tianjin, China*
[5]*Institute of Acute Abdominal Diseases, Integrated Traditional Chinese and Western Medicine, Tianjin Nankai Hospital, Tianjin, China*

Correspondence should be addressed to Yan Wang; wangyan@tjutcm.edu.cn and Lei Yang; nkyanglei@126.com

This study investigated the potential protective effects of alpha-mangostin (α-MG) on ultraviolet B (UVB)-induced damage in HaCaT cells. The results showed that α-MG less than $10\,\mu$M had no significant cytotoxicity and exposure to UVB ($50\,\text{mJ/cm}^2$) reduced cell viability by approximately 50% compared with the control. The $2\,\mu$M α-MG upregulated cell viability and downregulated the expression of metal matrix proteases (MMPs). The results of flow cytometry, real-time quantitative PCR (RT-qPCR), and immunoblotting manifested that α-MG relieved the extent of apoptosis and reduced the levels of apoptosis-associated mRNAs and proteins, respectively. The results of RT-qPCR and ELISA indicated that α-MG suppressed the generation of IL-6 and TNF-α. Furthermore, α-MG effectively downregulated activation of the UVB-induced nuclear factor κB (NF-κB) and mitogen-activated protein kinase (MAPK) signaling pathways. Finally, lipidomics profiling demonstrated that α-MG significantly reduced UVB radiation-increased ceramide. Overall, these results demonstrated that α-MG has beneficial effects against photoaging by reducing the ceramide content and inhibiting MAPK and NF-κB signaling pathways.

1. Introduction

There are various factors that affect the aging of the skin, such as ultraviolet (UV), air pollution, oxidative stress, and heredity, among which photoaging plays a principal role in skin aging, and skin photoaging approximately accounts for 80% in skin aging [1]. A major reason of skin photoaging is exposure to UV in sunlight, which alters the composition of skin cells and causes the loss of components of the extracellular matrix (ECM), thereby damaging the skin [2, 3]. The UV can be partitioned into three regions depending on different wavelengths, respectively, including ultraviolet A (UVA) (320–400 nm), ultraviolet B (UVB) (290–320 nm), and ultraviolet C (UVC) (200–290 nm). Since the great majority of UVC is absorbed by the ozone layer before reaching the earth, it can be concluded that the two critical types of UV that cause skin damage are UVA and UVB. In particular, UVB which is capable of causing skin sunburn has about 1000 times genotoxicity than UVA [4]. Constant exposure to UVB over a long period results in damages such as skin erythema, sunburn, oxidative damage, apoptosis, inflammation, and sometimes even skin cancer [2, 3, 5].

When HaCaT cells were irradiated by UVB, nuclear factor kappa B (NF-κB) and mitogen-activated protein kinase (MAPK) pathways were activated. The transcription factor of NF-κB is a heterodimer composed of the subunits of p50/p65. NF-κB induces the expression of inflammatory factors such as IL-6 and TNF-α through a cascade reaction in vivo, resulting in skin inflammation [6–8]. Since it has been reported that 12-HHT inhibits UVB-induced IL-6 synthesis via the negative regulation of P38 MAPK and the subsequent suppression of NF-κB activity [8]. MAPK belongs to the family of serine and tyrosine kinase, including extracellular signal-regulated kinase (ERK), c-Jun N-terminal kinase (JNK), and P38 MAPK, which are involved in cell multiplication, differentiation, apoptosis, and inflammation [8, 9]. In various cell apoptosis, overexpressed ceramides (Cers) may provoke apoptosis by directly participating in ROS generation through the modulation of MAPK signaling pathways [10–12]. These cascades of biochemical alterations ultimately lead to cells' death by diverse mechanisms, including B-cell lymphoma-2 (Bcl-2) depletion, Bcl-2-associated X protein (Bax) increase, and caspase-3 activation [9].

Alpha-mangostin (α-MG) is a major xanthone compound widely found in mangosteen pericarp [13]. It was confirmed to possess various bioactive functions including anti-inflammatory, antiapoptosis, anticancer, and antioxidant effects [14–16], and it has also been identified as an inhibitor of acid sphingomyelinase (ASM) [17]. ASM, which hydrolyzes sphingomyelin (SM) to Cers and phosphorycholine, is considered to be a key target of Cer production upon UV irradiation [18, 19]. α-MG improves endothelial dysfunction in diabetic mice through the inhibition of Cer [20]. Cers are important structural components of the epidermis, which plays a key role in maintaining homeostasis of the human body [20]. In addition, Cers also act as an active second messenger, regulate keratinocyte proliferation and differentiation, and enhance proinflammatory cytokines production [21]. Although study has shown that α-MG has an antiphotoaging effect [22], mechanisms of α-MG in protecting the skin from UVB damage still lack in-depth study. Therefore, we committed to studying the protective effect of α-MG for HaCaT cells against UVB irradiation and its potential molecular mechanism. This study aimed to provide both a theoretical and experimental basis for the development and application of α-MG; thereupon, a ceramide that is a prominent manifestation in the process of photoaging is disclosed.

2. Materials and Methods

2.1. Materials and Reagents.
α-MG (purity: HLPC $\geq$98%) (IM0500) and the IL-6 ELISA kit (SEKH-0013) were purchased from Solarbio (Beijing, China). The annexinV-FITC apoptosis assay kit was obtained from UE (T6013L, Suzhou, China). The reverse transcription kit was purchased from YEASEN (11150ES60, Shanghai, China), and Eastep™ qPCR Master Mix (2X) was purchased from Promega (LS2062, Beijing, China). The bicinchoninic acid (BCA) protein assay kit was provided by CWBIO (CW0014, Beijing, China).

Chloroform was of HPLC grade and was obtained from Honeywell (AH049-4, Morris Tow., USA). Methanol was of HPLC grade and was purchased from Fisher chemical (A452-4, Shanghai, China). Ammonium hydroxide solution was provided by Sigma-Aldrich (05002-1L, Missouri, USA). The UVB source employed is a Sigma SH4B light therapy device (Shanghai SIGMA High-tech Co., Ltd., Shanghai, China), with wavelength ranging between 311 and 313 nm and having a peak wavelength of 313 nm.

2.2. Cell Culture.
The HaCaT cells (CL-0090, Procell) were cultured in Dulbecco's modified eagle medium (DMEM) (Gibco, USA) supplemented with 10% fetal bovine serum (FBS, Biological Industries, Israel) and 1% penicillin-streptomycin (Gibco, USA) at 37°C in a humidified atmosphere aerated with 5% of CO_2.

2.3. UVB Irradiation and Administration.
Dissolve the appropriate amount of α-MG in DMSO to prepare a 10 mM stock solution and then directly dilute the stock solution to the appropriate concentration with DMEM (complete medium). HaCaT cells were allowed to grow an appropriate abundance and then the treatment group was treated with α-MG at a concentration of 2 μM. After 2 h, the complete culture medium of DMEM (complete medium) was substituted with PBS and then the cells were irradiated in UVB (50 mJ/cm^2). The PBS was removed after the UVB irradiation, and the culture of cells was sustained for 24 h in the complete medium for subsequent experiments. The control group was treated with the same conditions but without any exposure to UVB irradiation or α-MG treatment, whereas the UV group was irradiated with UVB but did not receive α-MG treatment.

2.4. Cell Viability.
After treatment, cells were incubated for 4 h in the culture medium with 10 μL of MTT (5 mg/mL). After removing the supernatant, 100 μL of DMSO was added into the complete DMEM. Finally, a plate reader (ST-360, Shanghai Kehua Biological Engineering Co., Ltd., Shanghai, China) was used to measure its absorbance at 490 nm.

2.5. Apoptosis.
After treatment, cells and supernatant were collected to assay the apoptosis rates. The annexinV-FITC apoptosis assay kit was used to perform the experiments following the manufacturer's instructions. Apoptotic and necrotic cells were measured using the EXFLOW flow cytometer (EXFLOW-206, Changzhou Bidake Biotechnology Co., Ltd., Jiangsu, China).

2.6. Real-Time Quantitative PCR (RT-qPCR).
After treatment, cells were collected and total RNA was extracted using TRIzol. After quality checking and purification, 2 μg of RNA was reverse transcribed to cDNA by using the reverse transcription kit. RT-qPCR was performed using SYBR Green Master Mix in a Bio-Rad IQ5 detection system. GAPDH is indexed as an internal reference, and at the same

time, three wells were set for each sample. The $2^{-\triangle\triangle Ct}$ method was used to calculate the relative content of mRNA. The upstream and downstream primer sequences of the gene are listed in Table 1.

2.7. Measurement of IL-6.

2.7. Measurement of IL-6. After treatment, supernatants of HaCaT cells were collected and centrifuged at 3,000 rpm for 10 min. The ELISA kit was used to measure IL-6 concentrations following the manufacturer's instructions. The absorbance (A450) was measured using a plate reader with a detection sensitivity of at least 1.0 pg/mL. The contents of IL-6 were calculated by interpolating the results onto a standard curve.

2.8. Immunoblotting. After treatment, cells were washed three times with PBS and collected in RIPA buffer for 30 min. The protein concentration was determined by using the BCA protein assay kit. After electrophoresis, the proteins were transferred to the polyvinylidene fluoride (PVDF) membrane (Millipore, Mass., USA). At a temperature of 4°C, we incubated the PVDF membrane with the following primary antibodies overnight: primary antibodies against GAPDH (AB0037, Abways Technology, 1:5000), p-P38 MAPK (9211, CST, 1:1000), P38 MAPK (9212, CST, 1:1000), p-JNK (9255, CST, 1:1000), JNK (9252, CST, 1:1000), p-ERK1/2 (8544, CST, 1:1000), ERK1/2 (4695, CST, 1:1000), p-NF-κB (3033, CST, 1:1000), NF-κB (8242, CST, 1:1000), Bax (2772, CST, 1:1000), Bcl-2 (3498, CST, 1:1000), and caspase-3 (9662, CST, 1:1000). Membranes were visualized using a chemiluminescence analyzer (Bio-Rad, USA). The relative density of the protein bands were analyzed by Quantity One software. The densitometry values were normalized by using GAPDH.

2.9. Lipidomics Profiling. After treatment, cells were collected. Lipids were extracted from cells using a modified Bligh and Dyer's extraction procedure (double rounds of extraction) and dried in the SpeedVac under the OH mode prior to analysis, and lipid extracts were resuspended in chloroform: methanol 1:1 (v/v) spiked with appropriate internal standards. All lipidomic analyses were carried out on an Agilent 1290 UPLC system coupled with a Sciex QTRAP 6500 PLUS system as described previously [23, 24]. Polar lipids were separated on a Phenomenex Luna Silica 3 μm column (i.d. 150 × 2.0 mm) under the following chromatographic conditions: mobile phase A (chloroform: methanol: ammonium hydroxide, 89.5:10:0.5) and mobile phase B (chloroform: methanol: ammonium hydroxide: water, 55:39:0.5:5.5) at a flow rate of 300 μL/min and column oven temperature at 30°C. Individual polar lipid species were quantified by referencing to spiked internal standards including SM-d18:1/12:0, Cer d18:1-d_7/15:0, GluCer-d18:1/8:0, and d3-LacCer-d18:1/16:0 obtained from Avanti Polar Lipids (Alabaster, AL, USA).

2.10. Statistical Analysis. All the data were shown as the mean ± standard deviation (SD) and processed using IBM SPSS Statistics 19 software. The two-independent-sample test was performed to assess differences between the two groups. A level of $P < 0.05$ indicated statistically significant.

3. Results and Discussion

3.1. Effect of α-MG and UVB on Cell Viability. The effect of different concentrations of α-MG (2, 4, 6, 8, 10, 15, and 20 μM) on the viability of HaCaT cells was assessed by the MTT method. The results showed that the IC_{50} value of α-MG was 19.17 μM on HaCaT cells, and there was no cytotoxicity when its concentration was inferior or equal to 10 μM (Figure 1(a)). The cell viability of cells irradiated with different UVB doses was assessed using the MTT assay. Like reported [25], we decided to create a cell model of photoaging under a median lethal irradiation intensity of 50 mJ/ cm^2 (Figure 1(b)).

To determine the potential protective effect that α-MG exerts on HaCaT cells, we performed MTT assay on HaCaT cells after exposure to UVB irradiation. After UVB exposure, the cell viability of HaCaT cells decreased strikingly. α-MG played a positive role in the proliferation of HaCaT cells. Compared with the UV group, α-MG at 2 μM enhanced viability of HaCaT cells by 10.24% (Figure 1(c)). These observations indicate that α-MG has protective effects in UVB-induced HaCaT cells.

3.2. α-MG Inhibits the Expression of MMPs. MMPs play a considerable role in the physiological mechanism of skin photoaging. The action of UV is to transform the connective tissue of the skin by upregulating the expressions of MMPs which degrade collagen and other ECM proteins [26, 27]. MMP-1 is a member of the MMPs in the collagenase family. After being activated, MMP-1 further degrades the collagens of type I and type III that has been degraded beforehand by MMP-2 and MMP-9, thereby provoking the degradation of collagen [26, 28]. Simultaneously, the gelatinolytic activity of MMP-9 is the central factor for skin damage and wrinkle formation due to UV [25, 29]. Therefore, the assessments on the expressions of MMPs have become preliminary in the process of screening agents against photoaging. In this study, we examined the mRNA levels of MMP-1, MMP-2, and MMP-9 through RT-qPCR. UVB irradiation dramatically increased the expressions of MMPs and α-MG treatment reversed this trend (Figures 1(d)–1(f)). This result indicates that α-MG prevents the loss of ECM and has a potential antiphotoaging effect. Thus, α-MG has the opportunity to be a candidate drug for the prevention and treatment of photoaging.

3.3. α-MG Inhibits Apoptosis. Apoptosis is a key factor of cell growth and homeostasis that maintain normal cell proliferation [30]. In this study, we explored the antiapoptotic properties of α-MG (Figure 2). As shown in Figures 2(a) and 2(b), UVB irradiation increased the percentage of apoptotic cells from 6.27% to 65.60%, which was remarkably reduced to 45.34% by α-MG. The results showed that pretreatment of HaCaT cells with α-MG was capable of attenuating apoptosis induced in UVB efficaciously.

TABLE 1: Sequence of primers used for RT-qPCR.

| Gene names	Forward primer (5′-3′)	Reverse primer (5′-3′)
IL-6	ACTCACCTCTTCAGAACGAATTG	CCATCTTTGGAAGGTTCAGGTTG
TNF-α	CCTCTCTCTAATCAGCCCTCTG	GAGGACCTGGGAGTAGATGAG
Bax	CCCGAGAGGTCTTTTTCCGAG	CCAGCCCATGATGGTTCTGAT
Bcl-2	GGTGGGGGTCATGTGTGTGG	CGGTTCAGGTACTCAGTCATCC
Caspase-3	CATGGAAGCGAATCAATGGACT	CTGTACCAGACCGAGATGTCA
MMP-1	AAAATTACACGCCAGATTTGCC	GGTGTGACATTACTCCAGAGTTG
MMP-2	CCCACTGCGGTTTTCTCGAAT	CAAAAGGGTATCCATCGCCAT
MMP-9	TGTACCGCTATGGTTACACTCG	GGCAGGGACAGTTGCTTCT
GAPDH	GGAGCGAGATCCCTCCAAAAT	GGCTGTTGTCATACTTCTCATGG
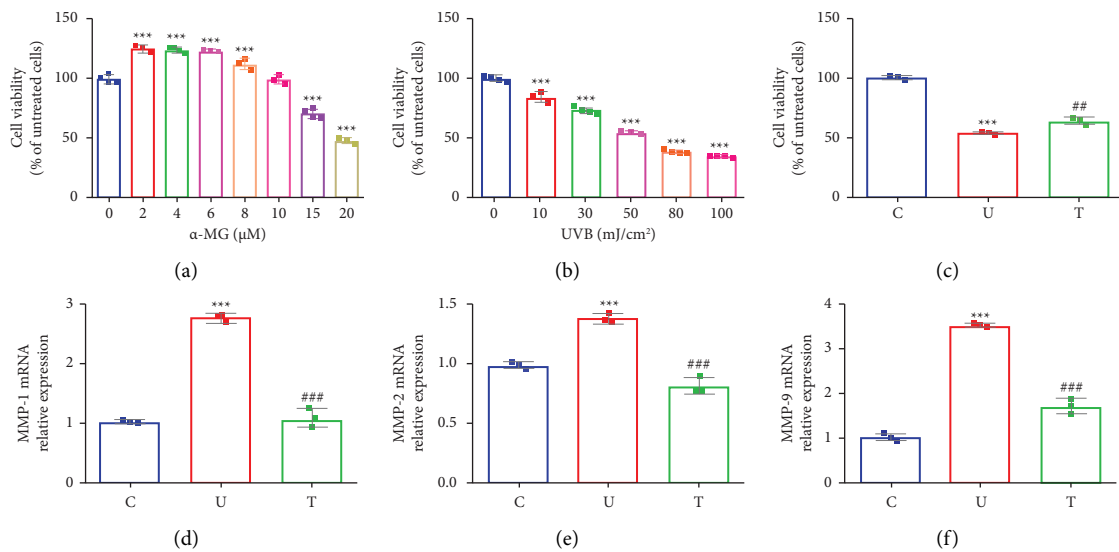
FIGURE 1: The protective effect of α-MG in UVB-induced HaCaT cells. (a) HaCaT cells were treated with 2–20 μM α-MG for 2 h and subsequent complete medium DMEM replacement drug solution continued incubation for 24 h, and cytotoxicity of α-MG was evaluated by the MTT assay. (b) HaCaT cells were treated with 10–100 mJ/cm^2, and cytotoxicity of UVB was evaluated by the MTT assay. (c) HaCaT cells were pretreated with or without α-MG (2 μM) for 2 h and then exposed to UVB (50 mJ/cm^2). At 24 h after UVB irradiation, cell viability was determined by the MTT assay. (d–f) MMP-1, MMP-2, and MMP-9 expressions were detected by RT-qPCR after α-MG pretreatment and then UVB irradiation (***$P < 0.001$ vs. the control group; ###$P < 0.001$ and ##$P < 0.01$ vs. the UV group; $n = 3$-4; C: control group; U: UV group; T: treatment group).

The activation of caspase-9 is the major initial step of the caspase-dependent endogenous apoptotic pathway [31]. Subsequently, downstream caspases or other caspases, including caspase-3, -6, and -7, are activated, eventually leading to cell death. The caspase substrate proteins are degraded in this process, which is the evidence of the induction of caspase-dependent apoptosis [31, 32]. The activation of caspase is manipulated by a variety of proteins, including members from the Bcl-2 family, such as Bcl-2 and Bax [32]. Therefore, the balance between the proapoptotic Bax and the antiapoptotic Bcl-2 plays a determinant role in activating cascade reaction through inducing or inhibiting caspase, thereby cascading to initiate the intrinsic apoptotic pathway. For the purpose of further exploring the inhibiting mechanism of α-MG inhibiting cell apoptosis, we used RT-qPCR and western blot to examine the mRNA and protein expression levels of Bcl-2, Bax, and caspase-3. As shown in Figures 2(c)–2(g), compared with the control group (C), the ratio of Bax/Bcl-2 and the expression of caspase-3 in the UV

group (U) were considerably increased. Compared with the U group, the ratios in the treatment group (T) were evidently decreased. The variations between mRNA and protein levels are consistent. The abovementioned results indicated that α-MG has an ability to resist UVB-induced apoptosis.

3.4. α-MG Decreases IL-6 and TNF-α Production.

Accumulating evidences indicate that after exposure to UVB, inflammatory response causes skin damage due to its stimulation on the secretion of inflammatory cytokines, including IL-6, TNF-α, and COX-2 [26, 33]. Similarly, in the present study, the HaCaT cells, one of the major targets of UVB, exhibited higher levels of proinflammatory cytokines when exposed to UVB. In addition, no matter what circumstances in which skin damage is caused, keratinocytes will be induced into excessive multiplication, which is closely related to the secretion of proinflammatory cytokines [34]. Therefore, it is of great significance to investigate the anti-
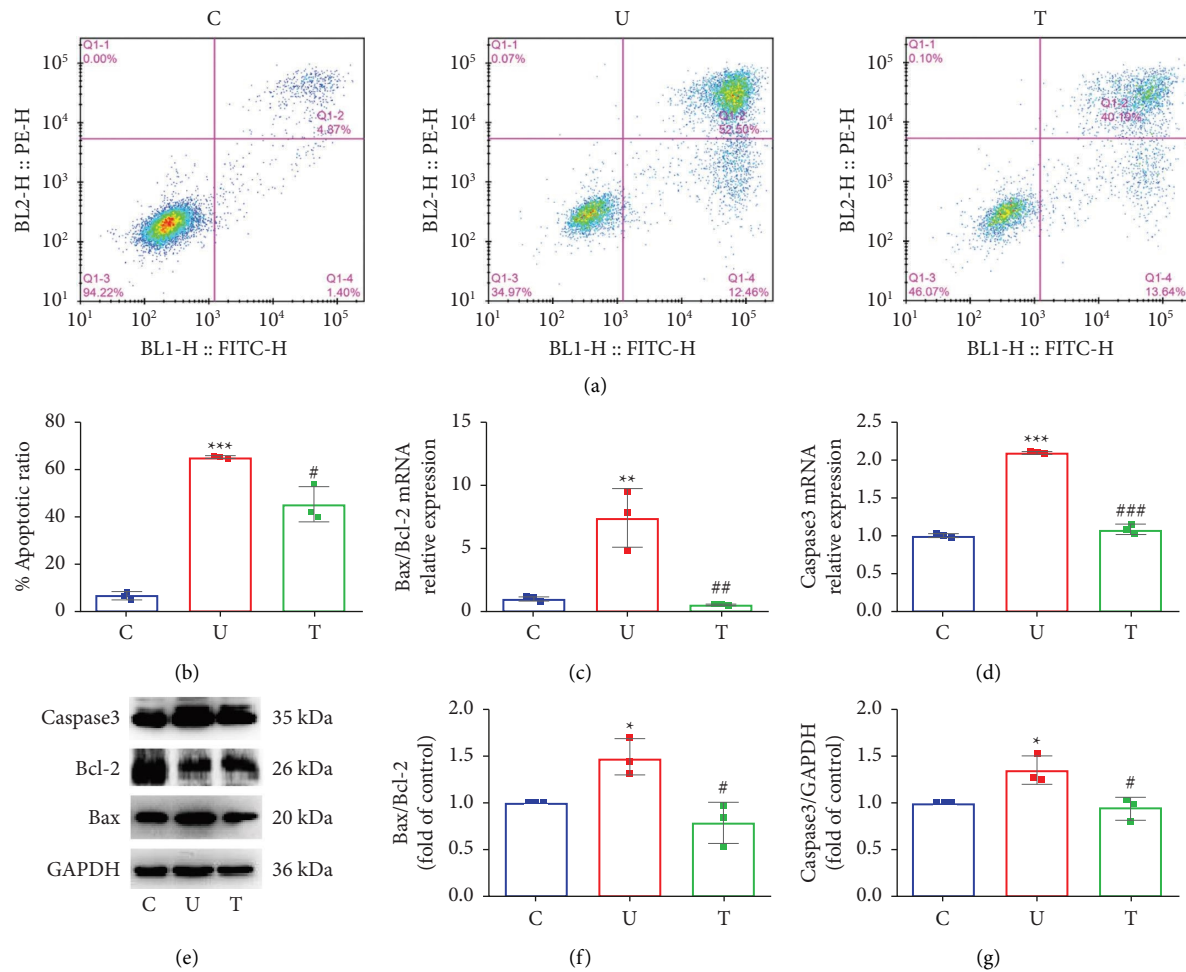
(a)

(b)

(c)

(d)

(e)

(f)

(g)

Figure 2: α-MG protects HaCaT cells against UVB-mediated apoptosis. (a, b) HaCaT cells were pretreated with or without α-MG ($2\,\mu$M) for 2 h and then exposed to UVB (50 mJ/cm^2). At 24 h after UVB irradiation, the cell apoptosis rate was determined by flow cytometry. (c, d) GAPDH as an internal control, the ratio of Bax/Bcl-2, and the expression levels of caspase-3 mRNA were presented. (e) After α-MG pretreatment and then UVB irradiation, Bcl-2, Bax, and caspase-3 were detected by western blot. (f, g) GAPDH as an internal control, the ratio of Bax/Bcl-2, and the expression levels of caspase-3 protein were presented ($^{***}P < 0.001$, $^{**}P < 0.01$, and $^{*}P < 0.05$ vs. the control group; $^{\#\#\#}P < 0.001$, $^{\#\#}P < 0.01$, and $^{\#}P < 0.05$ vs. the UV group; $n = 3$; C: control group; U: UV group; T: treatment group).

inflammatory effects of α-MG on UVB. α-MG protects HaCaT cells from inflammation in response to UVB radiation. The results demonstrated that the mRNA levels in IL-6 and TNF-α were remarkably upregulated in HaCaT cells upon UVB exposure, which were reversed by α-MG treatment (Figures 3(a) and 3(b)). ELISA experiments also confirmed the fact that α-MG reduced the content of IL-6 (Figure 3(c)). The abovementioned results indicated that α-MG could delay the process of skin inflammation through the anti-inflammatory effect. These results (Figures 1, 2, and 3(a)–3(c)) from multiple perspectives interpreted that α-MG provided a high degree of cytoprotection against UV irradiation-induced phototoxicity.

3.5. α-MG Inhibits NF-κB Activation and MAPK Phosphorylation. MAPK and NF-κB play pivotal roles in cellular responses to extracellular signals. Upon stimulation with predominantly pathological agents, MAPK modulates

the NF-κB activity by modulating its transactivation. The activated NF-κB complexes translocate from the cytoplasm to the nucleus and bind to the NF-κB target gene. Many studies have shown that UVB irradiation induces the activation of MAPK which can function as the upstream mediator of MMP-9 [35, 36]. It has also been reported that NF-κB increases MMP-9 expression in fibroblasts [37, 38]. Therefore, the phenomena of skin aging, such as UVB-induced MMP-9 expression, may be associated with the levels of phosphorylated MAPK and the activation of NF-κB.

It is well known that the NF-κB signaling pathway is also a classic inflammatory pathway, and it plays a major role in the production of proinflammatory cytokines in response to UVB irradiation. Our research showed that the increase in NF-κB phosphorylation induced by UVB irradiation was significantly decreased by α-MG (Figures 3(d)–3(f)). These suggest that α-MG exerts photoprotection through alleviating the inflammatory response to UVB irradiation by regulating NF-κB signaling.
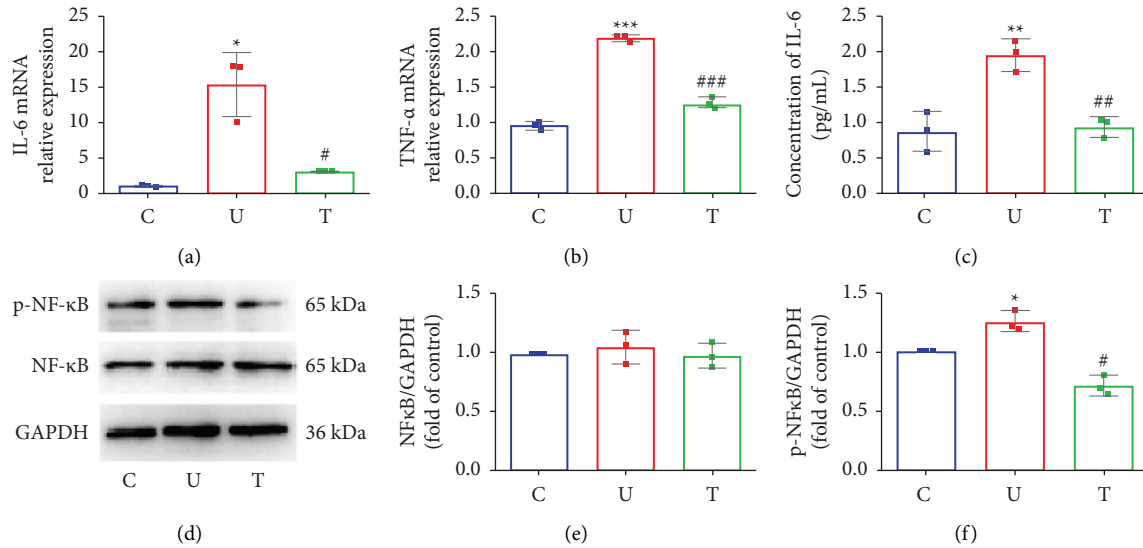
Figure 3: α-MG inhibited UVB-induced inflammatory reactions. (a, b) IL-6 and TNF-α expressions were detected by RT-qPCR after α-MG pretreatment and then UVB irradiation. (c) The content of IL-6 in the cell supernatant was detected by ELISA. (d) After α-MG pretreatment and then UVB irradiation, NF-κB and p-NF-κB were detected by western blot. (e, f) GAPDH as an internal control, the expression levels of NF-κB, and p-NF-κB proteins were presented ($^{***}P < 0.001$, $^{**}P < 0.01$, and $^{*}P < 0.05$ vs. the control group; $^{###}P < 0.001$, $^{##}P < 0.01$, and $^{#}P < 0.05$ vs. the UV group; $n = 3$; C: control group; U: UV group; T: treatment group).

The MAPK pathway-related proteins play a major role in the apoptosis and inflammation in response to UV irradiation [8, 9]. The increase in JNK, P38 MAPK, and ERK1/2 phosphorylation induced by UVB irradiation was significantly decreased by α-MG, and UVB and α-MG had no effect on nonphosphorylated JNK, P38 MAPK, and ERK1/2 (Figure 4). Taken together, these data demonstrate that α-MG protects HaCaT cells from UVB-induced apoptosis and inflammation by regulating MAPK signaling (Figures 2–4). This suggested the possibility that α-MG might attenuate photoaging-associated changes in vivo and suppress the inflammation of skin tissues.

3.6. α-MG Inhibits Cer Production. Lipids are important structural and functional components of the skin. Alterations in the lipid composition of the epidermis are associated with inflammation and apoptosis and can affect the barrier function of the skin [39, 40]. In this study, we investigated the changes in the lipid metabolism in HaCaT cells. By UPLC, we analyzed the molecular species of SM, Cer, glucosylceramide (GlcCer), and lactosylceramide (LacCer) in HaCaT cells in different groups. The numbers of lipid identifications are displayed in Figure 5(a). The lipid heat map analysis in HaCaT cells showed the following (Figure 5(b)): UVB irradiation leaded to an increase in the level of SM and its metabolites, such as Cer, GlcCer, and LacCer. After administration, the SM and Cer contents decreased and the content of GlcCer increased, while LacCer had no significant change. The research of Magnoni et al. showed that UVB irradiation increased the production of Cer in HaCaT cells, and there was a temporal correlation between the production of Cer and the apoptosis UVB-induced [41]. It was also detected that the activation of

neutral sphingomyelinase and ASM was activated when HaCaT cells were exposed to UVB [41]. Moreover, Okudaira found that α-MG inhibited ASM with an IC50 value of 14.1 μM (5.8 μg/mL) [17]. In this study, we observed that the content of Cer in the HaCaT cells UVB-induced increased. The administration of α-MG reversed this phenomenon. Combined with the changes of SM, GlcCer, and LacCer pre- or postadministration, it can be known that the degradation of SM was alleviated reducing the formation of Cer because α-MG inhibited the activity of ASM. In the meantime, the content of GlcCer (Cer derivative) still increased after administration. This indicates that under the intervention of α-MG, Cer tends to be converted into LacCer, thereby reducing its content. These results showed that after administration, α-MG on the one hand reduced the generation of Cer and on the other hand accelerated the conversion of Cer and ultimately reduced the level of Cer in HaCaT cells, protecting cells from damage caused by UVB irradiation.

Subsequently, we further analyzed the results and plotted a Venn diagram (Figure 5(c)) (U group vs. C group and T group vs. U group, $P < 0.05$). Notably, Cer d18:1/24:1 (a type of ceramide) had a biological significance in pairwise comparisons. The heat map of Cer (Figure 5(d)) and the relative content of Cer d18:1/24:1 (Figure 5(e)) once again confirmed the trend of Cer that UVB irradiation increased the content of Cer, and α-MG decreased the content of Cer. Cer, a lipid messenger, is one of the main mediators that regulate multiple pathways related to skin cell apoptosis and inflammation [18, 19]. UVB irradiated promoted cell apoptosis and aggravated the degree of inflammation, while the administration of α-MG reversed this phenomenon. It indicated that α-MG might inhibit cell apoptosis and inflammation in photoaging by reducing the content of Cer. It has also been reported that Cer is the upstream mediator of
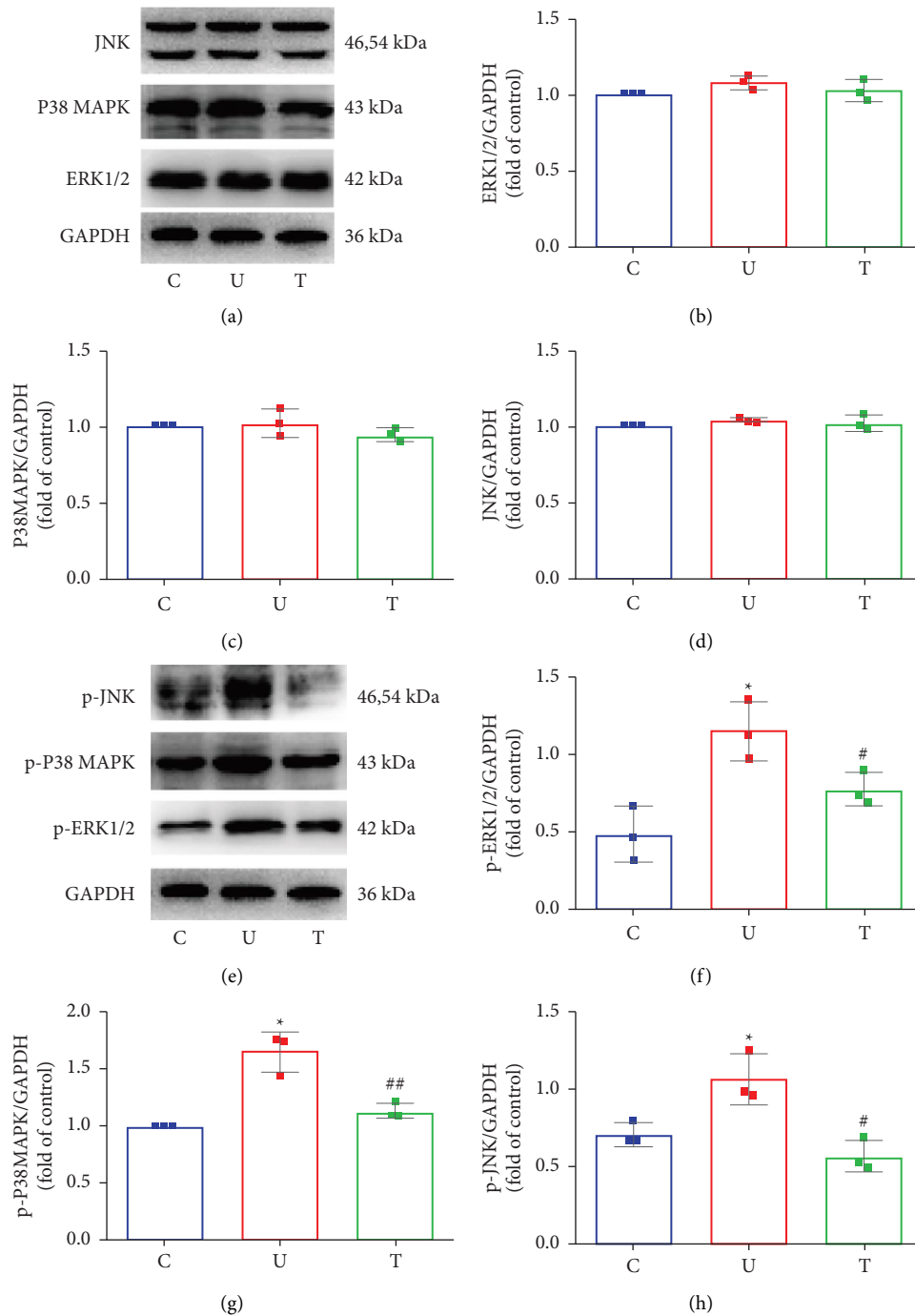
FIGURE 4: α-MG inhibited the phosphorylation of MAPK pathway proteins. (a, e) After α-MG pretreatment and then UVB irradiation, JNK, P38 MAPK, ERK1/2, p-JNK, p-P38 MAPK, and p-ERK1/2 were detected by western blotting. (b, d, f, h) GAPDH as an internal control and the expression levels of JNK, P38 MAPK, ERK1/2, p-JNK, p-P38 MAPK, and p-ERK1/2 proteins were presented ($^*P < 0.05$ vs. the control group; $^{##}P < 0.01$ and $^#P < 0.05$ vs. the UV group; $n = 3$; C: control group; U: UV group; T: treatment group).

MAPK [10–12]. Therefore, the activation of MAPK and NF-κB is related to the increase of Cer. Currently, research studies on Cer d18 : 1/24 : 1 basically focus on cardiovascular disease, diabetes, liver and kidney disease, and Alzheimer's disease [42–44]. In human keratinocytes, we disclosed its changes and effects for the first time. This provides a new target for other researchers to study skin photoaging.

Besides, Cer d18 : 1/24 : 1 is a biomarker of major adverse cardiovascular and cerebrovascular events (MACEs) [45]. However, this study lacks data to prove that it is a biomarker of skin photoaging.

In conclusion, the present study demonstrated the protective effects of α-MG on UVB-induced photoaging in HaCaT cells. α-MG has the potential to protect the skin
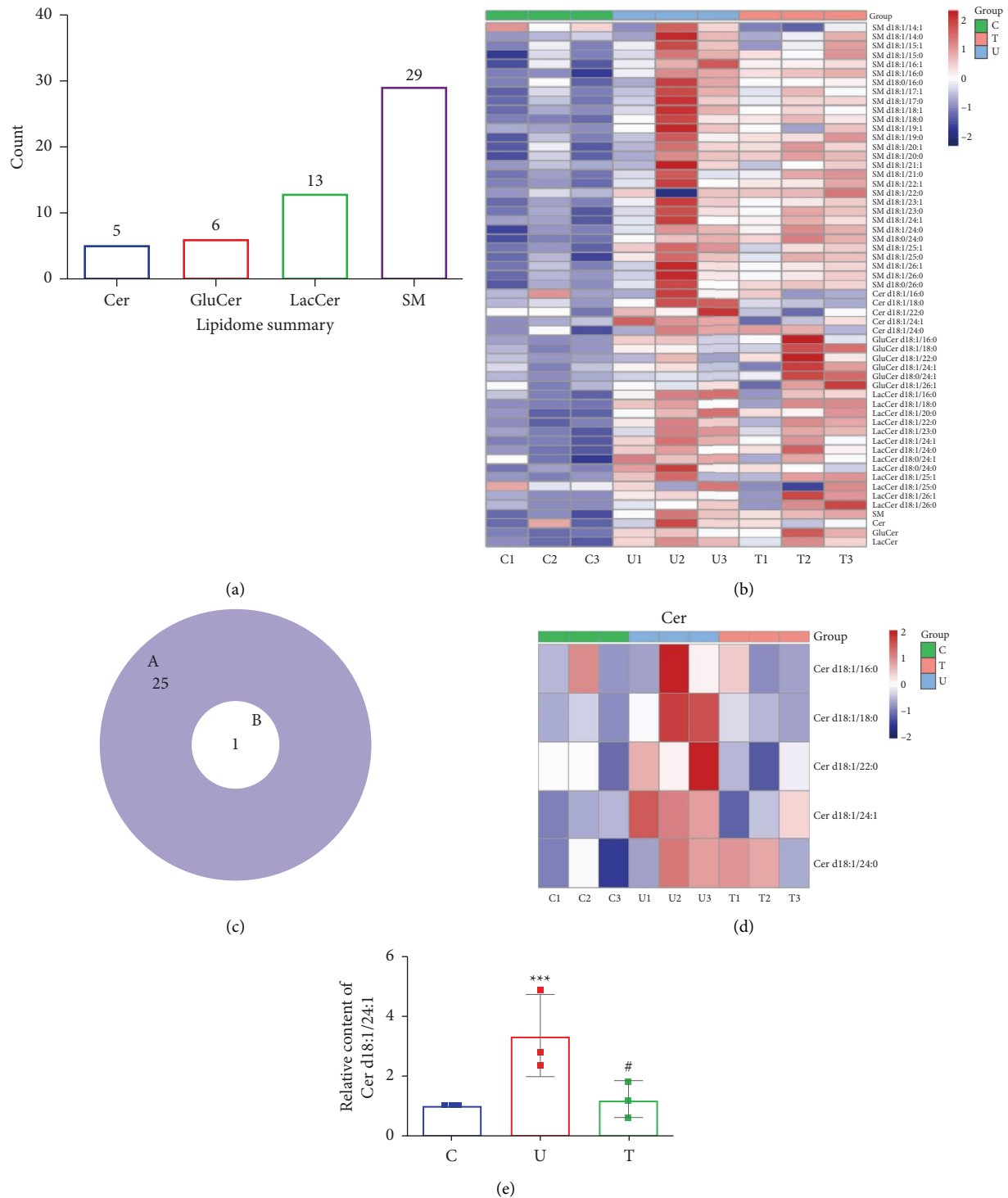
(a)

(b)

(c)

(d)

(e)

FIGURE 5: α-MG reduced the levels of Cer. (a) The metabolite statistics chart showed the 4 lipids of SM, Cer, GlcCer, and LacCer and their respective numbers. (b) After cluster analysis, the overall heat map of the four lipids in lipid metabolism was obtained. (c) The Venn diagram was obtained after further analysis. A represented U group vs. C group; B represented T group vs. U group; $P < 0.05$. 1 represented Cer d18 : 1/24 : 1. (d) After cluster analysis, the heat map of Cer was obtained. (e) The relative content of Cer d18 : 1/24 : 1 in each group was presented ($^{***}P < 0.001$ vs. the control group; $^{\#}P < 0.05$ vs. the UV group; $n = 3$; C: control group; U: UV group; T: treatment group).
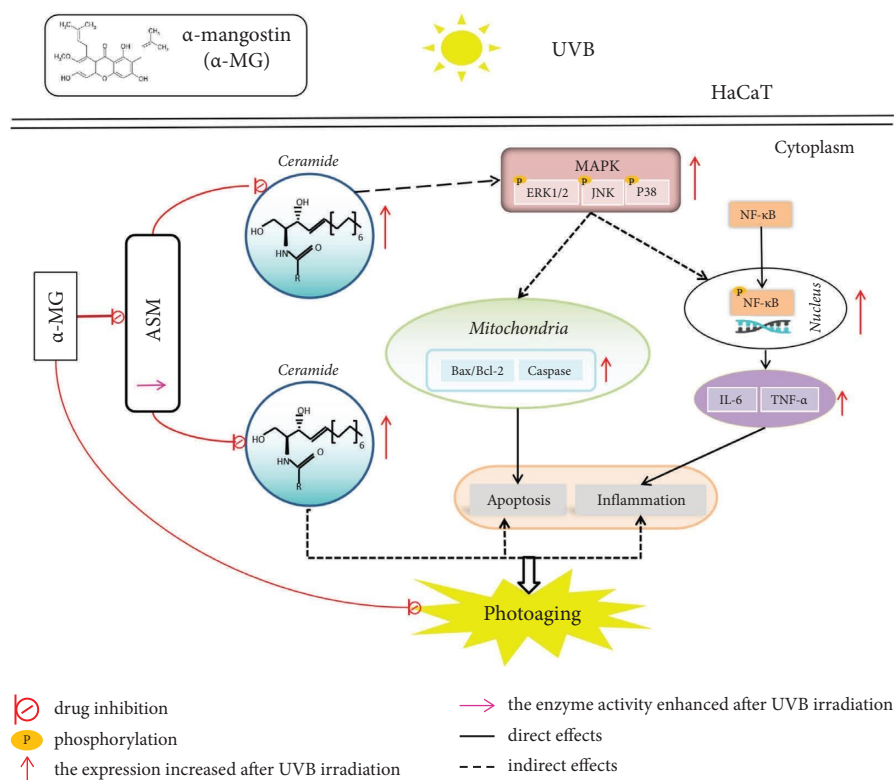
FIGURE 6: Molecular mechanism of α-MG resisting photoaging. Building on the confirmation of α-MG as an inhibitor of acid sphingomyelinase (ASM), we investigated its downstream mechanisms. After UVB irradiation of HaCaT cells, intracellular ceramide levels increased, leading to the activation of downstream MAPK and NF-κB pathways (phosphorylation of related proteins). This resulted in an increase in apoptosis-related protein expression (increased Bax/Bcl-2 ratio and caspase-3 content) and inflammatory factors (IL-6 and TNF-α), inducing cellular photoaging. The administration of α-MG could reverse these effects. The abovementioned results indicate that α-MG plays an antiapoptotic and anti-inflammatory role through ceramide, MAPK, and NF-κB signaling pathways, highlighting its potential to protect the skin from UVB-induced photoaging.

from UVB-induced photoaging, such as MMP-9 production, apoptosis-related proteins increase, and inflammatory factors production, possibly through the inactivation of ceramide-MAPK-NF-κB signaling pathways (Figure 6). The present study suggests that α-MG has a potential as therapeutic agents for the prevention and treatment of skin photoaging. However, because of the complex regulation of signaling pathways in cells, specific intermediates and intermolecular interactions need to be in-depth studied.

Data Availability

The data that support the findings of this study are available in the supplementary material of this article.

Additional Points

Practical Applications. Alpha-mangostin (α-MG) is a natural xanthone compound and one of the main active ingredients of agricultural mangosteen (*Garcinia mangostana L.*) pericarp. α-MG has been used as a botanical medicine for its potential health benefits considered as antioxidant, anti-inflammatory, anticancer, antiviral, and antibacterial and

has been attracting increasing research attention in recent years. Our research shows that α-MG has an antiphotoaging effect; thus, it can be used as an additive in the cosmeceutical industry to produce novel skin protectants. In addition, due to its antiapoptosis, anti-inflammatory, and MMP inhibitory effects, it can be used as a natural dietary supplement. Concomitantly, whole research provides a new approach for the recycle of mangosteen pericarp. Notably, Cer d18 : 1/24 : 1 (a type of ceramide), a biomarker of major adverse cardiovascular and cerebrovascular events (MACEs), was revealed for the first time in skin photoaging. This provides a new target for other researchers to study skin photoaging. In summary, the present study has confirmed that α-MG can be useful in therapeutic and cosmetic applications for the treatment of skin photoaging.

Conflicts of Interest

The authors declare that they have no conflicts of interest.

Authors' Contributions

Jiahui Jin and Yan Bao contributed equally to this work.

Acknowledgments

Supplementary Materials

Supplementary Material 1 related to Figures 1–4: the data in supplementary material 1 are the original data involved in experiments "2.3–2.8" of the "Materials and Methods" part. Supplementary Material 2 related to Figures 5: the data in supplementary material 2 are the original data involved in the experiment "2.9" of the "Materials and Methods" part. (*Supplementary Materials*)

References

[1] A. Kammeyer and R. M. Luiten, "Oxidation events and skin aging," *Ageing Research Reviews*, vol. 21, pp. 16–29, 2015.

[2] K. Murata, M. Oyama, M. Ogata, N. Fujita, and R. Takahashi, "Oral administration of Jumihaidokuto inhibits UVB-induced skin damage and prostaglandin E2 production in HR-1 hairless mice," *Journal of Natural Medicines*, vol. 75, no. 1, pp. 142–155, 2021.

[3] U. Muzaffer, V. I. Paul, B. Agilan, and N. R. Prasad, "Protective effect of Juglans regia L., against ultraviolet-B induced photoaging in human epidermal keratinocytes," *Biomedicine and Pharmacotherapy*, vol. 111, pp. 724–732, 2019.

[4] A. Svobodová, J. Psotová, and D. Walterová, "Natural phenolics in the prevention of UV-induced skin damage. A review," *Biomedical Papers*, vol. 147, no. 2, pp. 137–145, 2003.

[5] P. Lin, E. Hwang, H. T. Ngo, S. A. Seo, and T. H. Yi, "Sambucus nigra L. ameliorates UVB-induced photoaging and inflammatory response in human skin keratinocytes," *Cytotechnology*, vol. 71, no. 5, pp. 1003–1017, 2019.

[6] Y. Pan, Y. You, L. Sun et al., "The STING antagonist H-151 ameliorates psoriasis via suppression of STING/NF-κB-mediated inflammation," *British Journal of Pharmacology*, vol. 178, no. 24, pp. 4907–4922, 2021.

[7] Q. Li, H. Fang, E. Dang, and G. Wang, "The role of ceramides in skin homeostasis and inflammatory skin diseases," *Journal of Dermatological Science*, vol. 97, no. 1, pp. 2–8, 2020.

[8] J. W. Lee, H. C. Ryu, Y. C. Ng et al., "12(S)-Hydroxyheptadeca-5Z,8E,10E-trienoic acid suppresses UV-induced IL-6 synthesis in keratinocytes, exerting an anti-inflammatory activity," *Experimental and Molecular Medicine*, vol. 44, no. 6, pp. 378–386, 2012.

[9] T. Xiong, Z. Zhang, R. Zheng, J. Huang, and L. Guo, "N-acetyl cysteine inhibits lipopolysaccharide-induced apoptosis of human umbilical vein endothelial cells via the p38MAPK signaling pathway," *Molecular Medicine Reports*, vol. 20, no. 3, 2019.

[10] A. Zietzer, A. L. Jahnel, M. Bulic et al., "Activation of neutral sphingomyelinase 2 through hyperglycemia contributes to endothelial apoptosis via vesicle-bound intercellular transfer of ceramides," *Cellular and Molecular Life Sciences*, vol. 79, no. 1, p. 48, 2022.

[11] A. Rahman, S. Pallichankandy, F. Thayyullathil, and S. Galadari, "Critical role of H2O2 in mediating sanguinarine-induced apoptosis in prostate cancer cells via facilitating ceramide generation, ERK1/2 phosphorylation, and Par-4 cleavage," *Free Radical Biology and Medicine*, vol. 134, pp. 527–544, 2019.

[12] V. A. Movsesyan, A. G. Yakovlev, E. A. Dabaghyan, B. A. Stoica, and A. I. Faden, "Ceramide induces neuronal apoptosis through the caspase-9/caspase-3 pathway," *Biochemical and Biophysical Research Communications*, vol. 299, no. 2, pp. 201–207, 2002.

[13] A. Ghasemzadeh, H. Jaafar, A. Baghdadi, and A. Tayebi-Meigooni, "Alpha-mangostin-rich extracts from mangosteen pericarp: optimization of green extraction protocol and evaluation of biological activity," *Molecules*, vol. 23, no. 8, p. 1852, 2018.

[14] S. Y. Park, J. H. Lee, S. Y. Ko, N. Kim, S. Y. Kim, and J. C. Lee, "Antimicrobial activity of α-mangostin against *Staphylococcus* species from companion animals *in vitro* and therapeutic potential of α-mangostin in skin diseases caused by *S. pseudintermedius*," *Frontiers in Cellular and Infection Microbiology*, vol. 13, Article ID 1203663, 2023.

[15] T. Chavan and A. Muth, "The diverse bioactivity of α-mangostin and its therapeutic implications," *Future Medicinal Chemistry*, vol. 13, no. 19, pp. 1679–1694, 2021.

[16] F. Wang, H. Ma, Z. Liu, W. Huang, X. Xu, and X. Zhang, "α-Mangostin inhibits DMBA/TPA-induced skin cancer through inhibiting inflammation and promoting autophagy and apoptosis by regulating PI3K/Akt/mTOR signaling pathway in mice," *Biomedicine and Pharmacotherapy*, vol. 92, pp. 672–680, 2017.

[17] C. Okudaira, Y. Ikeda, S. Kondo et al., "Inhibition of acidic sphingomyelinase by xanthone compounds isolated from Garcinia speciosa," *Journal of Enzyme Inhibition*, vol. 15, no. 2, pp. 129–138, 2000.

[18] W. Luczaj, A. Jastrzb, M. D. R. Domingues, P. Domingues, and E. Skrzydlewska, "Changes in phospholipid/ceramide profiles and eicosanoid levels in the plasma of rats irradiated with UV rays and treated topically with cannabidiol," *International Journal of Molecular Sciences*, vol. 22, no. 16, 2021.

[19] H. Kashkar, K. Wiegmann, B. Yazdanpanah, D. Haubert, and M. Krönke, "Acid sphingomyelinase is indispensable for UV light-induced Bax conformational change at the mitochondrial membrane," *Journal of Biological Chemistry*, vol. 280, no. 21, pp. 20804–20813, 2005.

[20] M. Jiang, S. Huang, W. Duan, Q. Liu, and M. Lei, "Alpha-mangostin improves endothelial dysfunction in db/db mice through inhibition of aSMase/ceramide pathway," *Journal of Cellular and Molecular Medicine*, vol. 25, no. 7, 2021.

[21] Y. Uchida and K. Park, "Ceramides in skin health and disease: an update," *American Journal of Clinical Dermatology*, vol. 22, no. 6, pp. 853–866, 2021.

[22] A. R. Im, Y. M. Kim, Y. W. Chin, and S. Chae, "Protective effects of compounds from Garcinia mangostana L. (mangosteen) against UVB damage in HaCaT cells and hairless mice," *International Journal of Molecular Medicine*, vol. 40, no. 6, pp. 1941–1949, 2017.

[23] J. W. Song, S. M. Lam, X. Fan et al., "Omics-driven systems interrogation of metabolic dysregulation in COVID-19 pathogenesis," *Cell Metabolism*, vol. 32, no. 2, pp. 188–202, 2021.

[24] J. Lu, S. M. Lam, Q. Wan et al., "High-coverage targeted lipidomics reveals novel serum lipid predictors and lipid pathway dysregulation antecedent to type 2 diabetes onset in normoglycemic Chinese adults," *Diabetes Care*, vol. 42, no. 11, pp. 2117–2126, 2019.

[25] Z. Xiao, P. Liang, J. Chen et al., "A peptide YGDEY from Tilapia gelatin hydrolysates inhibits UVB-mediated skin photoaging by regulating MMP-1 and MMP-9 expression in

HaCaT cells," *Photochemistry and Photobiology*, vol. 95, no. 6, pp. 1424–1432, 2019.

[26] B. Cui, Y. Wang, J. Jin et al., "Resveratrol treats UVB-induced photoaging by anti-MMP expression, through anti-inflammatory, antioxidant, and antiapoptotic properties, and treats photoaging by upregulating VEGF-B expression," *Oxidative Medicine and Cellular Longevity*, vol. 2022, Article ID 6037303, 19 pages, 2022.

[27] S. Liu, L. You, Y. Zhao, and X. Chang, "Hawthorn polyphenol extract inhibits UVB-induced skin photoaging by regulating MMP expression and type I procollagen production in mice," *Journal of Agricultural and Food Chemistry*, vol. 66, no. 32, pp. 8537–8546, 2018.

[28] H. Laronha and J. Caldeira, "Structure and function of human matrix metalloproteinases," *Cells*, vol. 9, no. 5, p. 1076, 2020.

[29] H. S. Kim, J. H. Song, U. J. Youn et al., "Inhibition of UVB-induced wrinkle formation and MMP-9 expression by mangiferin isolated from Anemarrhena asphodeloides," *European Journal of Pharmacology*, vol. 689, no. 1-3, pp. 38–44, 2012.

[30] J. Saegusa, D. K. Hsu, W. Liu et al., "Galectin-3 protects keratinocytes from UVB-induced apoptosis by enhancing AKT activation and suppressing ERK activation," *Journal of Investigative Dermatology*, vol. 128, no. 10, pp. 2403–2411, 2008.

[31] B. Tummers and D. R. Green, "Caspase-8: regulating life and death," *Immunological Reviews*, vol. 277, no. 1, pp. 76–89, 2017.

[32] Y. Kiraz, A. Adan, M. Kartal Yandim, and Y. Baran, "Major apoptotic mechanisms and genes involved in apoptosis," *Tumor Biology*, vol. 37, no. 7, pp. 8471–8486, 2016.

[33] C. C. Chen, A. N. Chiang, H. N. Liu, and Y. T. Chang, "EGb-761 prevents ultraviolet B-induced photoaging via inactivation of mitogen-activated protein kinases and proinflammatory cytokine expression," *Journal of Dermatological Science*, vol. 75, no. 1, pp. 55–62, 2014.

[34] T. Sugawara, R. M. Gallucci, P. P. Simeonova, and M. I. Luster, "Regulation and role of interleukin 6 in wounded human epithelial keratinocytes," *Cytokine*, vol. 15, no. 6, pp. 328–336, 2001.

[35] C. Song, L. R. Lorz, J. Lee, and J. Y. Cho, "In vitro photoprotective, anti-inflammatory, moisturizing, and antimelanogenic effects of a methanolic extract of chrysophyllum lucentifolium cronquist," *Plants*, vol. 11, no. 1, p. 94, 2021.

[36] T. Chen, H. Hou, Y. Fan et al., "Protective effect of gelatin peptides from pacific cod skin against photoaging by inhibiting the expression of MMPs via MAPK signaling pathway," *Journal of Photochemistry and Photobiology B: Biology*, vol. 165, pp. 34–41, 2016.

[37] R. G. Daré, M. M. Oliveira, M. C. T. Truiti, C. V. Nakamura, V. F. Ximenes, and S. O. S. Lautenschlager, "Abilities of protocatechuic acid and its alkyl esters, ethyl and heptyl protocatechuates, to counteract UVB-induced oxidative injuries and photoaging in fibroblasts L929 cell line," *Journal of Photochemistry and Photobiology, B: Biology*, vol. 203, Article ID 111771, 2020.

[38] R. Karthikeyan, G. Kanimozhi, N. R. Prasad et al., "7-Hydroxycoumarin prevents UVB-induced activation of NF-κB and subsequent overexpression of matrix metalloproteinases and inflammatory markers in human dermal fibroblast cells," *Journal of Photochemistry and Photobiology, B: Biology*, vol. 161, pp. 170–176, 2016.

[39] L. Li, C. Cataisson, B. Flowers et al., "Topical application of a dual ABC transporter substrate and NF-κB inhibitor blocks multiple sources of cutaneous inflammation in mouse skin," *Journal of Investigative Dermatology*, vol. 139, no. 7, pp. 1506–1515.e7, 2019.

[40] Y. Jia, Y. Gan, C. He, Z. Chen, and C. Zhou, "The mechanism of skin lipids influencing skin status," *Journal of Dermatological Science*, vol. 89, no. 2, pp. 112–119, 2018.

[41] C. Magnoni, E. Euclidi, L. Benassi et al., "Ultraviolet B radiation induces activation of neutral and acidic sphingomyelinases and ceramide generation in cultured normal human keratinocytes," *Toxicology in Vitro*, vol. 16, no. 4, pp. 349–355, 2002.

[42] A. Mantovani, A. Csermely, E. Sani et al., "Association between higher circulating leucine-rich α-2 glycoprotein 1 concentrations and specific plasma ceramides in postmenopausal women with type 2 diabetes," *Biomolecules*, vol. 12, no. 7, p. 943, 2022.

[43] S. Schmidt, S. F. Gallego, I. D. Zelnik et al., "Silencing of ceramide synthase 2 in hepatocytes modulates plasma ceramide biomarkers predictive of cardiovascular death," *Molecular Therapy*, vol. 30, no. 4, pp. 1661–1674, 2022.

[44] A. Mantovani, S. Bonapace, G. Lunardi et al., "Association of plasma ceramides with myocardial perfusion in patients with coronary artery disease undergoing stress myocardial perfusion scintigraphy," *Arteriosclerosis, Thrombosis, and Vascular Biology*, vol. 38, no. 12, pp. 2854–2861, 2018.

[45] L. P. de Carvalho, S. H. Tan, G. S. Ow et al., "Plasma ceramides as prognostic biomarkers and their arterial and myocardial tissue correlates in acute myocardial infarction," *JACC: Basic to translational science*, vol. 3, no. 2, pp. 163–175, 2018.